International Journal of
Molecular Sciences

MDPI

Article

Metabolite Patterns in Human Myeloid Hematopoiesis Result from Lineage-Dependent Active Metabolic Pathways

Lars Kaiser [1,2], Helga Weinschrott [1], Isabel Quint [1], Markus Blaess [1], René Csuk [3], Manfred Jung [2,4], Matthias Kohl [1] and Hans-Peter Deigner [1,5,6,*]

1 Institute of Precision Medicine, Medical and Life Sciences Faculty, Furtwangen University, Jakob-Kienzle-Straße 17, 78054 Villingen-Schwenningen, Germany; kal@hs-furtwangen.de (L.K.); weh@hs-furtwangen.de (H.W.); qui@hs-furtwangen.de (I.Q.); markus.blaess@web.de (M.B.); kohl@hs-furtwangen.de (M.K.)
2 Institute of Pharmaceutical Sciences, University of Freiburg, Albertstraße 25, 79104 Freiburg i. Br., Germany; manfred.jung@pharmazie.uni-freiburg.de
3 Organic Chemistry, Martin-Luther-University Halle-Wittenberg, Kurt-Mothes-Str. 2, 06120 Halle (Saale), Germany; rene.csuk@chemie.uni-halle.de
4 CIBSS—Centre for Integrative Biological Signalling Studies, University of Freiburg, 79104 Freiburg, Germany
5 Fraunhofer Institute IZI, Leipzig, EXIM Department, Schillingallee 68, 18057 Rostock, Germany
6 Associated member of Tuebingen University, Faculty of Science, Auf der Morgenstelle 8, 72076 Tübingen, Germany
* Correspondence: Hans-Peter.Deigner@hs-furtwangen.de; Tel.: +49-7720-307-4232

Received: 24 July 2020; Accepted: 21 August 2020; Published: 24 August 2020

Abstract: Assessment of hematotoxicity from environmental or xenobiotic compounds is of notable interest and is frequently assessed via the colony forming unit (CFU) assay. Identification of the mode of action of single compounds is of further interest, as this often enables transfer of results across different tissues and compounds. Metabolomics displays one promising approach for such identification, nevertheless, suitability with current protocols is restricted. Here, we combined a hematopoietic stem and progenitor cell (HSPC) expansion approach with distinct lineage differentiations, resulting in formation of erythrocytes, dendritic cells and neutrophils. We examined the unique combination of pathway activity in glycolysis, glutaminolysis, polyamine synthesis, fatty acid oxidation and synthesis, as well as glycerophospholipid and sphingolipid metabolism. We further assessed their interconnections and essentialness for each lineage formation. By this, we provide further insights into active metabolic pathways during the differentiation of HSPC into different lineages, enabling profound understanding of possible metabolic changes in each lineage caused by exogenous compounds.

Keywords: myeloid hematopoiesis; hematotoxicity; metabolite patterns; lineage commitment; active metabolic pathways; metabolome screening; hematopoietic stem cell differentiation

1. Introduction

Assessment of toxic properties from environmental or xenobiotic compounds remains a major field of research. Mammalian laboratory animals are currently considered as the "gold standard" in toxicology [1]. However, as mammalian models are expensive and time-consuming, several in vitro models have been developed and applied [2–4]. Indeed, models based on primary human cells are currently believed to more accurately reflect in vivo responses towards selected compounds, even though their applicability is partially restricted by limited life span and the necessity for cell

isolation prior to experiment [1,5]. In addition to the usage of primary cells, significant advances have also been achieved in the field of tissue engineering, a promising approach in approximating in vitro results to observed in vivo responses [6–9]. Current research sets a special focus on primitive cell types (e.g., embryonal stem cells, induced pluripotent cells), as these are appreciated to be particularly vulnerable towards exogenous stimuli and also display a model for developmental toxicity testing [10–13]. In this regard, models based on hematopoietic stem and progenitor cells (HSPC) are often used for the assessment of possible hematotoxic properties of compounds. Assessment of hematotoxicity, in fact, is of notable interest, as hematopoiesis continuously occurs during an individual's whole lifetime and large quantities of all blood cells arise daily from hematopoietic stem cells. Furthermore, as several environmental contaminants are known to cross the placenta, fetal HSPC are of particular interest, as these display potential sentinels of later-life hematopoietic disorders [14]. To date, traditional hematotoxicity testing is performed using colony forming unit (CFU) assays, however, also more lineage-specific models have recently been developed [15,16].

Identification of the toxicological mode of action of single compounds is of particular interest, as this often enables transferability of results across different tissues sharing similar metabolic characteristics. Several techniques have already been applied successfully for identification of the corresponding mode of action of various compounds, including molecular modeling or microarray-based approaches for assessment of carcinogenicity [17,18]. Currently, omics technologies are useful for identifying such features in common, as these enable rapid and wide screening [19]. Metabolomics presumably displays the most promising approach, as it is thought to display the phenotype most accurately together with prediction of toxic effects at very early stages [20]. Currently, two general approaches are used in the field of metabolomics, namely targeted (mass spectrometry (MS)-based) and nontargeted (nuclear magnetic resonance spectroscopy (NMR)- or high-resolution mass spectrometry (HRMS)-based) analysis. The selection of method depends on several variables, such as the scope of the planned analysis or the available type of sample material [21,22]. While NMR-based approaches in general do not depend on extensive sample preparation, the methods are less sensitive, compared to (HR)MS-based analysis [21]. A significant flaw of metabolomics, however, is the need for large amounts of sample material (typically $>1 \times 10^6$ cells per replicate), making metabolomics mostly incompatible for large screening approaches with the aforementioned hematopoietic models [23–27]. Sample size may be reduced by restricting the tested set to abundant metabolites, usage of sophisticated equipment or extensive sample preparation [27–32]. Nevertheless, profound knowledge of the total cellular metabolism in the different lineages is a prerequisite for interpretation of observed metabolic changes, as it ultimately defines the response of cells towards different stimuli [33,34]. As an example, intracellular levels of NADPH define the response to reactive oxygen species (ROS)-inducing compounds. Intracellular levels of NADPH in turn, depend on pentose phosphate pathway (PPP) activity, as well as on the activity of *IDH1* and *ME1* [35,36]. Thus, two cell types differing in their PPP activity may exhibit distinct responses towards the same compound, rendering profound knowledge of active metabolic pathways an essential feature for understanding.

In the context of hematotoxicity, cell type-specific effects are already well-appreciated, several compounds are known to induce lineage-specific effects. For example, erythroid progenitors are known to be more susceptible against lead, benzene or N-acetylcysteine than other lineages [15,37–39]. In the case of 3'-azido-3'-deoxthymidine (Azidothymidin), this cell type-specific effect is even more pronounced; erythroid progenitors are substantially reduced, while granulocyte/macrophage as well as megakaryocytic progenitors remain unaffected [40]. In addition, it also should be noted, that endogenous compounds may possess an impact on hematopoiesis as well. For example, lactate was shown recently to promote erythropoiesis via induction of ROS [41]. Such effects may be identified by usage of classical colony-forming unit (CFU) assays or more recently developed hematopoietic differentiation models [16]. For elucidation of the mode of action behind such effects, however, profound knowledge of the similarities and differences in the metabolism of each lineage is essential. Likewise, identification of relations between active metabolic pathways and specific responses likely

enables prediction of similar response patterns to other compounds with analogical modes of actions. Moreover, such relations may also enable prediction of response patterns across different tissues, leading to a better prediction of possible tissue-specific and toxic effects during drug development or the testing of xenobiotics.

Indeed, lineage-dependent regulatory involvement of single metabolic pathway activity during hematopoiesis is quite evident. Regulation of fatty acid oxidation (FAO) for instance, seems to be crucial for hematopoietic stem cell (HSC) maintenance, since blocking of FAO promotes HSC commitment [42]. However, autophagy-mediated generation of free fatty acids and subsequent degradation via FAO is crucial for neutrophil differentiation, indicating active FAO during differentiation of (at least) some lineages [43]. Furthermore, lymphocytes, neutrophils and macrophages utilize glutamine at high rates under catabolic conditions (e.g., sepsis), underlining the importance of glutaminolysis during HSPC differentiation [44]. Blocking glutaminolysis in erythropoietin (EPO)-stimulated HSPC, however, leads to a shift from erythroid commitment towards a myelomonocytic fate [45]. Therefore, modulation of glutaminolysis by xenobiotic compounds may also result in lineage-specific toxicity. Nevertheless, the assumption that glutaminolysis solely defines erythroid lineage commitment falls quite short, since it has been shown recently that blocking choline generation from phosphatidylcholine also impairs erythroid differentiation [46]. The role of phosphatidylcholine degradation within differentiation of other myeloid lineages, however, remains vague. In addition, several studies suggest a relation of polyamines with erythroid differentiation, their role in other lineages, however, again remains inconclusive [47–49]. Taken together, the essentialness of several different metabolic pathways during defined HSPC differentiation has already been shown for selected lineages. The general activities and interconnections between the different metabolic pathways, also within other lineages, however, still remains unclear. Therefore, a direct comparison of active metabolic pathways within different hematopoietic lineages is desirable in order to further elucidate the mode of action behind possible lineage-specific effects.

Here, we combined a known HSPC expansion approach with distinct lineage differentiations from the literature, resulting in formation of erythrocytes, dendritic cells (DC) and neutrophils. Due to the initial expansion step, large cell numbers can be generated with this approach, making it highly suitable for omics-based toxicity testing (e.g., demonstrated in [50]). Further assessment of metabolic and transcriptional changes during lineage formation resulted in unique and common metabolite sets, reflecting distinct metabolic changes in several interconnected pathways (namely glycolysis, glutaminolysis, polyamine synthesis, fatty acid oxidation and synthesis, as well as glycerophospholipid and sphingolipid metabolism). We further assessed the essentialness of glutaminolysis, polyamine synthesis and FAO for differentiation of each lineage, confirming the proposed activities. While several pathways were active in different lineages, interconnections between the distinct pathways were found to be unique for each lineage, while one of such interconnections was essential for erythrocytes. Taken together, we here established an HSPC differentiation model, suitable for metabolic toxicity screening and assessed the unique combination of active metabolic pathways, as well as their interconnections for each lineage, enabling the understanding of differing metabolic changes in myeloid hematopoiesis, caused by exogenous compounds.

2. Results

2.1. Expansion Approach Preserves Restricted Myeloid-Lineage Potential

As MS-based quantification of metabolites typically requires a large amount of biological material, we applied an initial expansion step of $CD34^+$ HSPC. The applied protocol led to a total expansion of alive cells by 286 ± 46-fold after 13 days (Figure 1B) [51]. However, only around 45.65% ± 1.88% of total cells remained $CD34^+$ positive (independent of CD38 expression) after expansion, also primitive markers as CD135 and CD45RA largely remained negative while a large part of the population indicated CD90 positive (Figure 1A). Nevertheless, many typical lineage markers remained negative,

only around 10.42% ± 2.04% were CD235a positive (Supplemental Figure S1A) [52]. Indeed, primitive HSC are often determined as CD34 $^{+}$ CD38^{-}, representing only a minor fraction of the here generated population [14]. However, as the CD34 $^{+}$ CD38^{+} population displayed a variety of further differentiated progenitors (e.g., common myeloid progenitors), still owning multilineage differentiation potential, the total amount of CD34^{+} cells (termed progenitor population) was assessed [14]. In brief, these results indicate that the differentiation of primitive progenitors occurs during expansion, a lack of most lineage markers, however, indicates a multilineage potential in the expanded population.

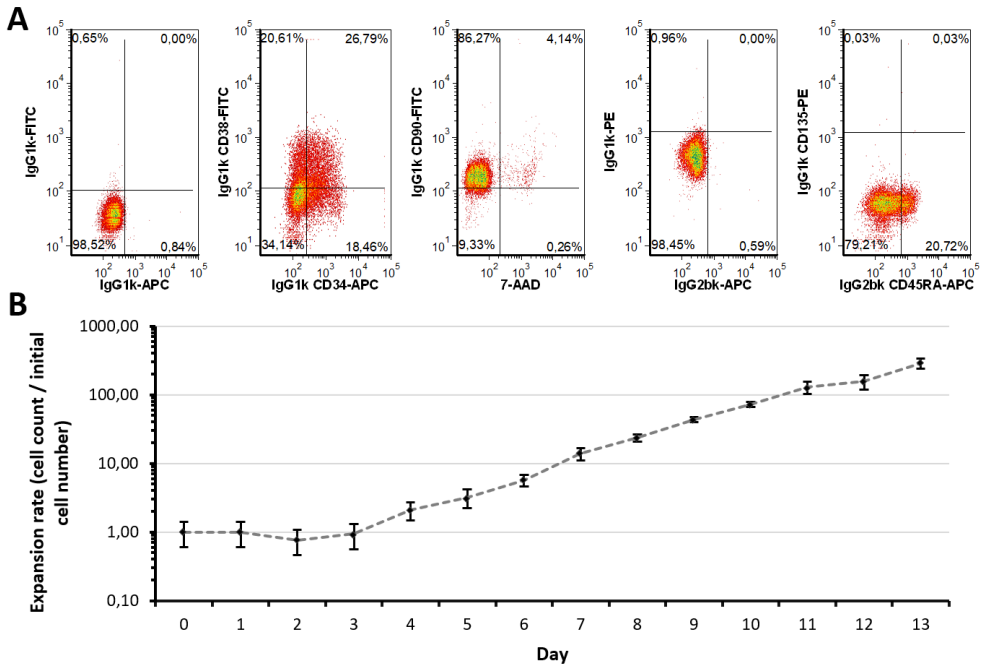

Figure 1. Characteristics of expanded CD34^{+} HSPC population. (**A**) Expression of HSPC surface markers in the progenitor population in comparison to corresponding isotype controls. Representative dot plots from three independent experiments (n = 3) are shown. (**B**) Growth characteristics of CD34^{+} HSPC during the expansion phase. Data are represented as mean ± SD (n = 3). Alive cell numbers were determined by trypan blue exclusion method, using a hemacytometer.

We therefore continued differentiation of the progenitor population into erythroid [53], megakaryocytic [54] and natural killer T cell lineages [55]. Erythroid differentiation could be confirmed (Figure S1B) while lineage markers for megakaryocytic and natural killer T cell lineages remained negative (Figure S1C,D). Assessment of further lineage markers, however, revealed that CD1a^{+} dendritic cells (Figure S1C) and CD66b^{+} neutrophils (Figure S1D) were formed as major populations. This observation is also supported by transcriptomic data, as several of the most extensively expressed genes could be matched to the afore mentioned lineages (Table S1). As *HBB* and *TFRC* are both erythroid, *ELANE*, *S100-A8*, *PRTN3* and *AZU1* are neutrophil markers, *GPNMB* is expressed by antigen-presenting cells (APC), *MRC1* and *C1QC* by macrophages and DC, while *EPX* is expressed by eosinophils, the expression patterns indicate, that the main lineages formed are erythrocytes, DC as well as neutrophils [56–60]. Furthermore, gene ontology enrichment analysis of the generated populations also support this assumption, as most significantly upregulated biological processes include erythrocyte differentiation and homeostasis for the erythroid population, as well as biological processes related to immune response for the other populations (Table 1).

Table 1. Gene ontology enrichment analysis, using the Fisher's exact test type in combination with Holm adjusted *p* value, from the differentiated lineages. The five most significantly enriched biological processes in each lineage are shown.

Biological Process	Fold Enrichment	Holm Adjusted *p* Value
Erythrocytes		
Immune system process	2.19	0.00009
Cytokine-mediated signaling pathway	3.50	0.00174
Response to chemical	1.81	0.00282
Erythrocyte differentiation	11.25	0.00355
Erythrocyte homeostasis	10.12	0.00771
Dendritic Cells		
Immune response	2.76	$< 10^{-10}$
Immune-system process	2.35	$< 10^{-10}$
Leukocyte activation involved in immune response	4.34	$< 10^{-9}$
Cell activation involved in immune response	4.31	$< 10^{-9}$
Leukocyte activation	3.59	$< 10^{-9}$
Neutrophil Granulocytes		
Defense response	4.09	$< 10^{-27}$
Immune response	3.47	$< 10^{-26}$
Immune system process	2.77	$< 10^{-24}$
Immune effector process	4.20	$< 10^{-22}$
Myeloid cell activation involved in immune response	5.98	$< 10^{-20}$

Taken together, these data demonstrate the multi-lineage potential of the generated progenitor population as it was possible to form erythroid, DC, neutrophil and eosinophil lineages. Since all populations reside in the myeloid branch of hematopoiesis, we assume that the progenitor population either consists of restricted myeloid progenitor cells or of a mixture of further differentiated progenitors. Indeed, transcriptomics data also indicate that other lineages are formed within each population, however, the main lineages formed are erythrocytes, DC as well as neutrophils, as verified via flow cytometry.

2.2. Myeloid Lineages Display Several Unique and Common Metabolic Patterns during Differentiation Accompanied by Changes in Pathway-Related Genes

Based on the successful identification of each main lineage formed, we performed global targeted metabolome profiling, testing for 514 metabolites in total. We totally identified 173 metabolites being altered from the progenitor population in the mature lineages (Figure 2A). In this set, 81 metabolites were significant in erythrocytes, 99 metabolites in DC and 73 in neutrophils (Supplemental Tables S2–S4). While several metabolic changes seemed to be comparable between two or more populations, several unique changes were present (Figure 2A). By applying criteria for identification of the unique and common changes (as stated in the methods section), we found 17 unique metabolites changed in erythrocytes (Figure 2A highlighted with red, Supplemental Table S5), 14 unique metabolites in DC (Figure 2A highlighted with green, Supplemental Table S6) and 46 unique metabolites in neutrophils (Figure 2A highlighted with blue, Supplemental Table S7). When these unique metabolic changes were directly compared in all three lineages, a cluster for each lineage was clearly visible (Figure 2B). Several metabolite changes in fact were found in common, with erythrocytes and DC displaying the largest overlap with 25 metabolites (Figure 2A highlighted with yellow, Supplemental Table S8). Common metabolites between the other combinations of populations, however, were rather rare (Figure 2A highlighted with cyan, pink and black, Supplemental Tables S9–S11).

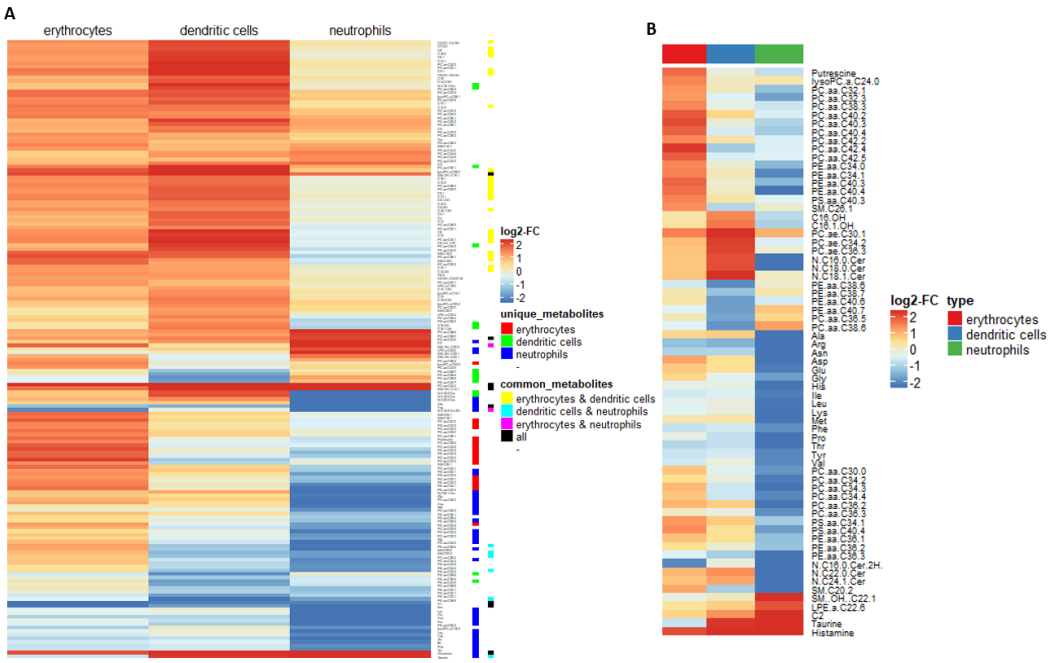

Figure 2. Biologically relevant metabolite changes in each differentiated lineage and identified unique metabolite patterns. (**A**) Biologically relevant metabolite changes in each differentiated lineage (for a detailed list of metabolites and their allocation, see Supplemental Table S13). (**B**) Unique metabolite patterns in each differentiated population. The mean $\log_2$ fold change, in comparison to the progenitor population, of the identified unique metabolites is displayed ($n = 3$). Biologically relevant, unique and common metabolites were identified as stated in the materials and methods section.

As we sought to identify the underlying changes on metabolic pathway levels, we analyzed the expression of enzymes, related to the relevant metabolites. Whole pathway activity is often regulated by a small number of key enzymes (e.g., hexokinase, phosphofructokinase and pyruvate kinase in glycolysis), therefore, whole pathway activity can often be derived from the expression of these in combination with metabolite concentrations [61]. Furthermore, as enzyme activity is tightly controlled via several mechanisms, including expression, we omitted FDR-correction of the p value in order to avoid an increase of the type II error (false negatives) [62]. By using this approach, we found several transcriptional changes, related to the corresponding metabolic pathways (Table 2).

Table 2. Transcriptional changes in pathway-related genes in each population. Given is gene name, the corresponding metabolic pathway and the $\log_2$ fold change, compared to the progenitor population. Changes with a corresponding p value > 0.05 were considered not significant (n.s.).

Gene	Metabolic Pathway	Erythrocytes	Dendritic Cells	Neutrophils
SLC2A1	Glycolysis	1.69	n.s.	n.s.
SLC2A5		n.s.	n.s.	1.94
SLC2A6		n.s.	n.s.	2.28
HK3		1.77	2.65	3.76
MINPP1		0.96	−1.47	n.s.
PKLR		4.42	n.s.	n.s.
FBP1		n.s.	4.44	5.36
OAT	Polyamine synthesis	0.95	n.s.	n.s.
ODC		n.s.	−1.89	−1.47
SAT1		n.s.	1.28	1.16
MYC		1.19	n.s.	n.s.

Table 2. *Cont.*

Gene	Metabolic Pathway	Erythrocytes	Dendritic Cells	Neutrophils
ME1	NADPH production	n.s.	2.88	n.s.
IDH1		n.s.	1.97	n.s.
CPT1a	FA oxidation	n.s.	n.s.	−1.25
FASN	FA biosynthesis	1.10	n.s.	n.s.
ACSL1		n.s.	1.14	n.s.
ELOVL6	FA elongation	1.41	n.s.	n.s.
THEM5		n.s.	n.s.	Inf
SCD	Biosynthesis of unsaturated FA	1.13	1.36	n.s.
LIPA	Lipolysis	n.s.	2.86	2.75
PLD3	Glycero-phospholipid metabolism	0.96	2.54	2.33
PLBD1		1.84	n.s.	3.118
PLA2G15		n.s.	1.24	n.s.
PLA2G16		n.s.	n.s.	2.73
LPCAT3		1.09	n.s.	n.s.
PISD		1.03	n.s.	n.s.
PHOSPHO1		3.91	n.s.	n.s.
PPAP2B		−2.28	1.73	2.54
LPIN1		n.s.	n.s.	-Inf
PCYT1B		n.s.	-2.02	−2.40
PLA2G7	Ether lipid metabolism	1.41	4.18	3.34
SPTSSB	Sphingolipid metabolism	3.11	5.07	n.s.
ACER3		n.s.	1.14	n.s.
SMPD3		Inf	n.s.	Inf
PPAP2B		−2.28	1.73	2.54

2.3. Myeloid Lineages Own a Higher Hexose Consumption with Different Fate

As the energy metabolism seems to play a crucial role during HSPC maintenance and differentiation, we focused on glycolysis, FAO and glutaminolysis, as these display the three major pathways for energy transformation [63]. Hexoses were found to be strongly reduced in all lineages (Supplemental Table S12), also expression of corresponding transmembrane transporters (*SLC2A1*, *SLC2A5* and *SLC2A6*) was either upregulated or unchanged (Table 2), indicating that lowered hexoses are related to raised catabolic reactions. This interpretation is further supported by the increased expression of *HK3* in all lineages. Expression of *PKLR*, however, was upregulated in erythrocytes, while *FBP1* was upregulated in DC and neutrophils. As *PKLR* catalyzes the formation from phosphoenolpyruvate to pyruvate, it can be concluded that erythrocytes own higher consumption of hexoses, subsequently used for the Krebs cycle. It has, however, been shown that nucleotide synthesis from glucose-6-phosphate (G6P) via the PPP is vital for erythroid differentiation [45]. However, we could not detect any difference in the expression of enzymes related to the PPP, indicating that erythrocytes use G6P under native conditions for further catabolic breakdown via glycolysis, as well as for nucleotide biosynthesis via PPP. *FBP1* catalyzes the back conversion of fructose 1,6-bisphosphate to fructose 6-phosphate (F6P), acting as the rate-limiting enzyme in gluconeogenesis. As F6P readily can be converted to G6P, we assume that both lineages primarily use glucose for nucleotide biosynthesis and ROS production from NADPH via PPP, which is also supported by findings of other groups [64,65].

2.4. Combined Fatty Acid Generation and Respective Fate Is Unique for Each Myeloid Lineage

Several acylcarnitines were raised in erythrocytes and DC, 18 of which could be defined as changes common to both lineages (Supplemental Tables S3, S4 and S9). Only three acylcarnitines, however, were increased in the neutrophil lineage, with acetylcarnitine concentration being uniquely affected (Supplemental Tables S5 and S8). Acylcarnitines serve as a carnitine shuttle for fatty acids through the mitochondrial membranes, while even-chain acylcarnitines and hydroxylated species result from β-oxidation, odd-chain species from α-oxidation and dicarboxylated species from ω-oxidation [66–69]. It is well-known, that acylcarnitines can also play a role in maintaining free CoA availability, whilst also reflecting corresponding acyl-CoA concentrations within the cell [67]. As the activity of FAO was demonstrated in HSC and during neutrophil differentiation, it is reasonable to assume that both possess enhanced FAO [43,63]. We therefore assume, that raised acylcarnitines indicate a lower FAO, which is also supported by the fact that species, resulting from α- and ω-oxidation, are raised as well. As α- and ω-oxidation only take place at substantial amounts if β-oxidation is disturbed, this further indicates reduced FAO [70,71].

Conversely, we found expression of *CPT1a* lowered in the neutrophil lineage (Table 2). As transesterification by *CPT1a* is one of the rate-limiting steps in FAO, this decreased expression seemed contradictory to our assumptions. However, usage of etomoxir as an irreversible inhibitor of *CPT1* only affected neutrophil differentiation (Figure 3A,D and Figure 4B,C), confirming our hypothesis of active FAO in neutrophils. Surprisingly, addition of etomoxir during neutrophil differentiation led to a higher expression of *ELANE* (Figure 3D). As etomoxir effectively reduced the proportion of $CD11b^+$ cells during neutrophil differentiation, our results seemed rather conflicting [43]. However, *ELANE* and CD11b are both expressed at different stages during neutrophil maturation, while *ELANE* is expressed in promyelocytes and myelocytes; CD11b expression starts in metamyelocytes [72,73]. Furthermore, expression of *ELANE* is inversely correlated to the maturation of neutrophils [72,74]. Therefore, we concluded that the higher expression of *ELANE* in etomoxir-treated populations indicated an enrichment of promyelocytes and myelocytes. In line with this assumption, the expression of *S100A8*, correlating with neutrophil maturation, was lowered by increasing amounts of etomoxir (Figure 3E) [74]. Thus, FAO seemed to be essential for neutrophil maturation, as already previously observed [43]. Nevertheless, formation of committed progenitors seemed to be independent of FAO. This interpretation, however, awaits further confirmation by future studies.

Interestingly, C16-OH and C16:1-OH acylcarnitines were uniquely raised in DC, but not in erythrocytes (Figure 2B, Supplemental Table S8). In fact, intracellular fatty acids (FA) and corresponding acyl-CoA species can result from catabolic reactions via lipolysis, as well as from anabolic reactions via FA synthesis. We found expression of *FASN* and *ELOVL6* uniquely stimulated in the erythrocyte lineage, while expression of *LIPA* was enhanced in DC and neutrophils. Furthermore, we found *ACSL1* elevated in DC and *THEM5* in neutrophils, also *SCD* was elevated in erythrocytes and DC.

Summarized, these results indicate that erythrocytes perform higher FA synthesis, while both, DC and neutrophils, perform higher lipolysis of cholesteryl esters (CE) and triglycerides (TG). FAs are further catabolized via FAO in neutrophils, while erythrocytes and DC seem to utilize FAs for anabolic processes. Erythrocytes, however, preferably elongate C16:0 and C16:1 FAs (Figure 5), which leads to diminished concentrations of these FAs, which, in turn, is reflected by corresponding acyl-CoAs and thus acylcarnitines.

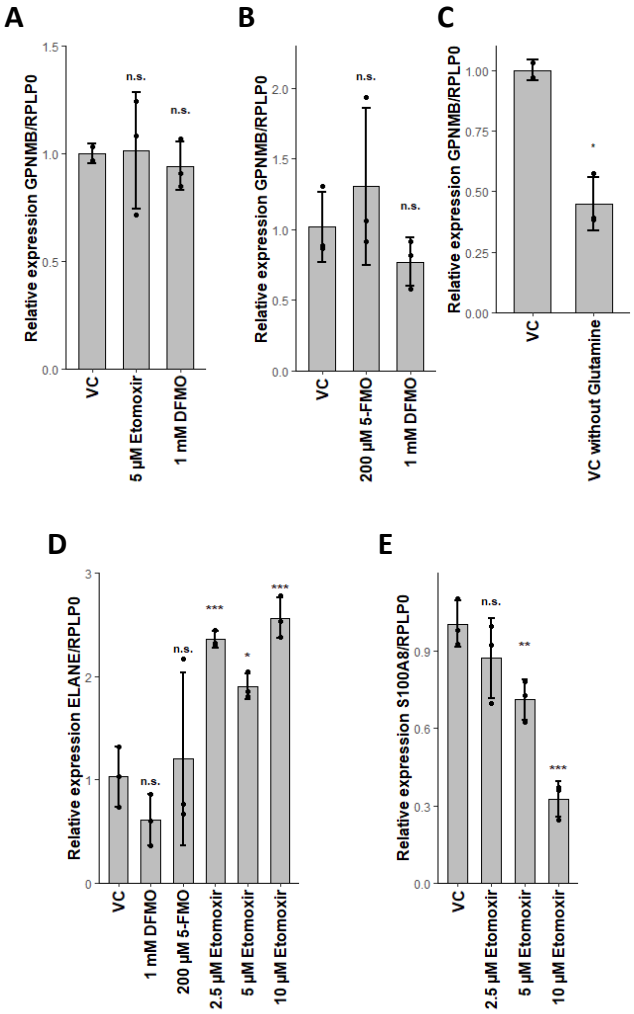

Figure 3. Glutaminolysis is essential during dendritic cell differentiation, while fatty acid oxidation is essential for neutrophil maturation. (**A**) Effect of etomoxir or difluormethyl-ornithine (DFMO) in the presence of glutamine on GPNMB/RPLP0 expression of dendritic cells. (**B**) Effect of 5-fluoromethylornithine (5-FMO) or DFMO in the absence of glutamine on GPNMB/RPLP0 expression of dendritic cells. (**C**) Effect of glutamine on GPNMB/RPLP0 expression of dendritic cells. (**D**) Effect of 5-FMO, DFMO or etomoxir in the presence of glutamine on ELANE/RPLP0 expression of neutrophils. (**E**) Effect of etomoxir in the presence of glutamine on S100A8/RPLP0 expression of neutrophils. Data are represented as mean ± SD ($n = 3$). Relative gene expression was calculated as stated in the methods section. Significant changes were assessed by one-way ANOVA (n.s. not significant; * $p < 0.05$; ** $p < 0.01$; *** $p < 0.001$).

2.5. Glutaminolysis Crosstalk with FAO and Its Interconnection to Polyamine Synthesis in Erythrocytes

In context to glutamine metabolism, we found uniquely lowered levels of the products Glu, Asn, Asp, Ala and Pro in neutrophils (Figures 2B and 5). As it is known that glutaminolysis is critical to erythroid differentiation, we assume that both erythrocytes and DC perform glutaminolysis [45]. This assumption was further supported by the reduced GPNMB expression in DC upon glutamine depletion (Figure 3C). In erythrocytes, however, glutamine depletion only reduced the cell expansion rate, HBB expression remained unaffected (Figure 4H,I). Glutaminolysis, therefore, seems to be crucial for DC differentiation, however, in erythrocytes, it appears to be beneficial for cell expansion, but not for maturation. In neutrophils, however, we assume that high ATP production by FAO concomitantly leads to reduced free phosphate levels, which in turn lead to lowered glutaminase activity [75].

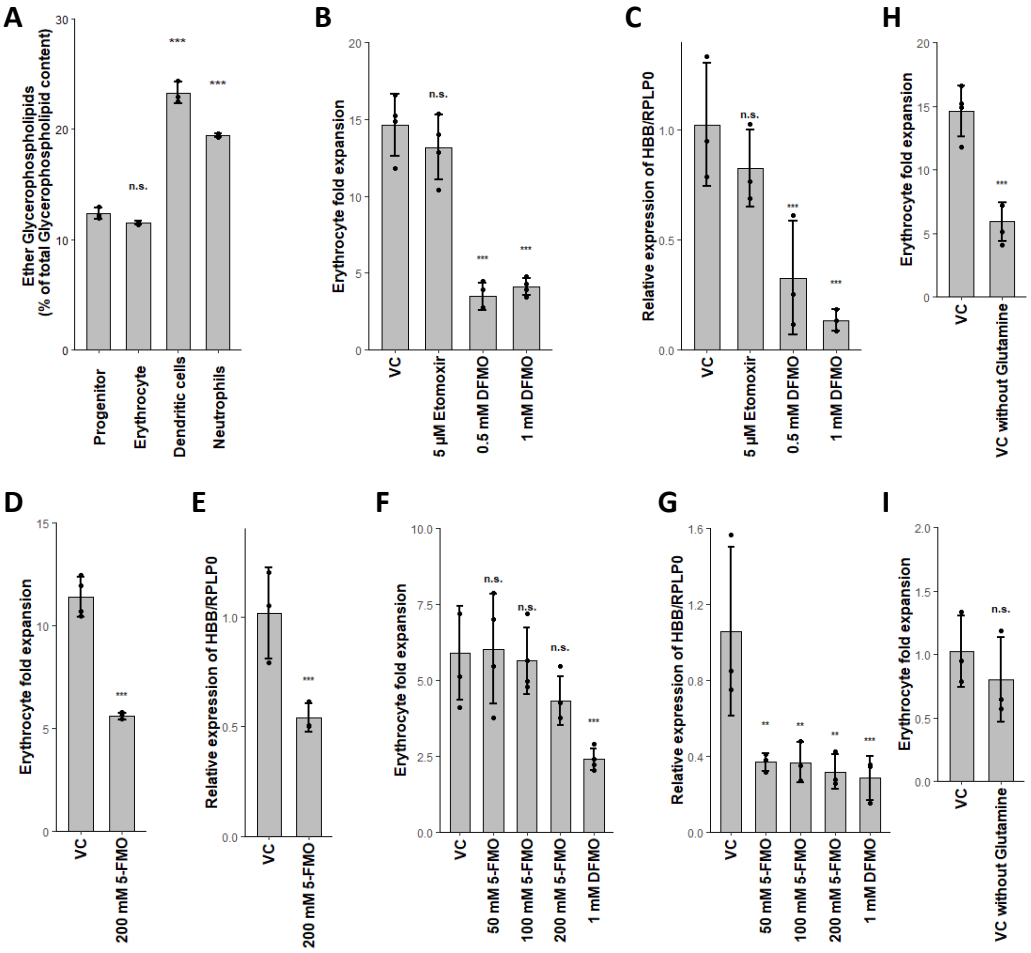

Figure 4. Polyamine synthesis and glutamine metabolism are both essential for erythropoiesis and interconnected via *OAT*. (**A**) Percentual content of ether lipids. (**B**,**C**) Effect of etomoxir or difluormethyl-ornithine (DFMO) in the presence of glutamine on erythroid expansion and relative HBB/RPLP0 expression. (**D**,**E**) Effect of 5-fluoromethylornithine (5-FMO) in the presence of glutamine on erythroid expansion and relative HBB/RPLP0 expression. (**F**,**G**) Effect of 5-FMO or DFMO in the absence of glutamine on erythroid expansion and relative HBB/RPLP0 expression. (**H**,**I**) Impact of glutamine on erythroid cell expansion and relative HBB/RPLP0 expression. Data are represented as mean ± SD (n = 3 for ether lipid content and gene expression, n = 4 for cell expansion). Percentual content of lipids, expansion rates and relative gene expression was calculated as stated in the methods section. Significant changes were assessed by one-way ANOVA (n.s. not significant; ** $p < 0.01$; *** $p < 0.001$).

Interestingly, we found *ME1* and *IDH1* raised in DC, both resulting in NADPH generation from Krebs cycle intermediates (Table 2) [35]. Cross-regulation between glycolysis and FAO via NADPH and acetyl-CoA is well-known, furthermore, pyruvate is generated via *ME1* [76]. We therefore assume, that in DC, FAO is mainly negatively regulated by glutaminolysis and not glycolysis (Figure 5).

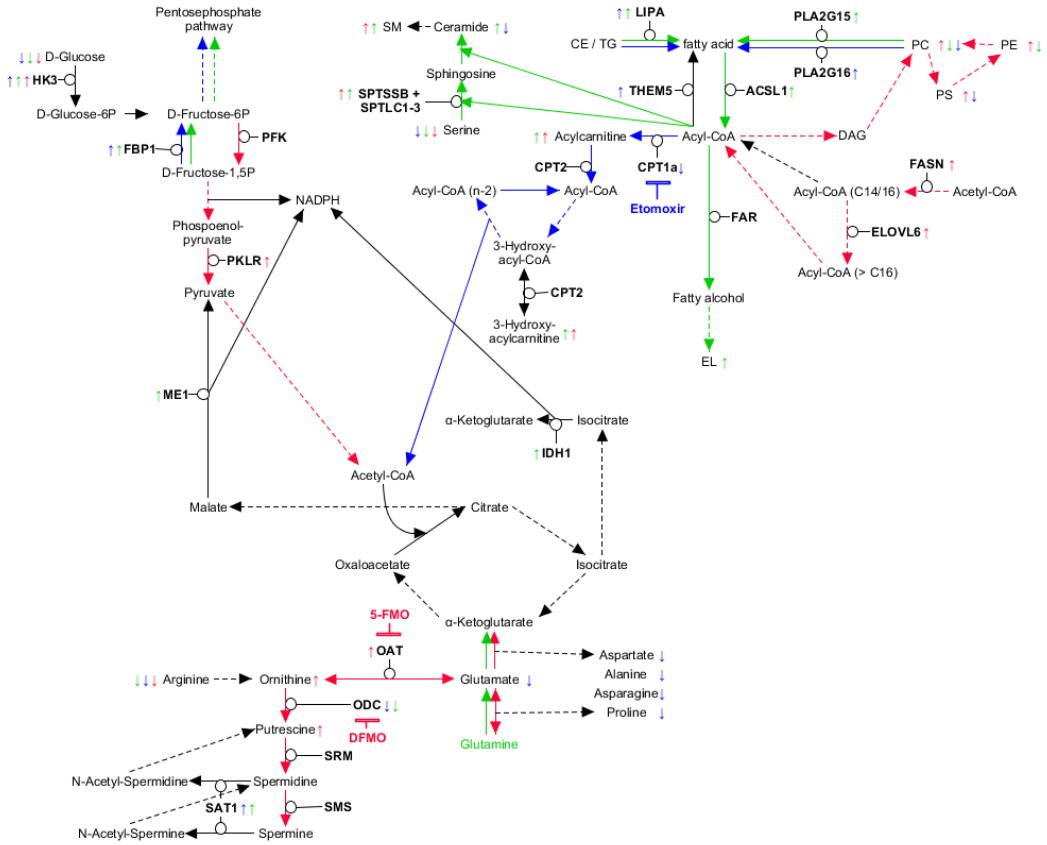

Figure 5. Involvement of unique metabolites in interconnected metabolic pathways. Model depicting the interconnection of key reactions of glycolysis, Krebs cycle, glutaminolysis, FAO and lipid metabolism. Differences in concentrations and proposed activities found are highlighted for neutrophils (blue), dendritic cells (green) and erythrocytes (red). Furthermore, inhibitors (DFMO, 5-FMO, Etomoxir) are indicated in the respective color of the lineage, affected by the corresponding inhibitor. The model was generated using KEGG pathways as the template [77].

Furthermore, we found putrescine concentrations uniquely increased in erythroid differentiation (Figure 2B, Supplemental Table S6), while downstream metabolites spermidine and spermine remained unaffected. Orn was elevated in erythrocytes whilst not fulfilling the criteria as a unique metabolite, whereas Arg was lowered in all lineages (Figure 2B, Supplemental Tables S3, S8 and S12). We further found *ODC* expression reduced in DC and neutrophils, while *SAT1* was raised (Table 2). Polyamine levels in fact have been reported to be relatively high in erythrocytes, confirming our observations [78]. This pattern indicates that the anabolism of polyamines is stable during erythroid differentiation, resulting in raised putrescine levels, whilst being diminished during DC and neutrophil differentiation. Several reasons may account for this: it is well-known that polyamines are important in regulating gene expression, as they are mostly bound to RNA and are essential for cell cycle progression [49]. As such they are found at higher concentrations in high proliferating cells. Further, polyamines have been found to inhibit the trans-bilayer movement of phospholipids and reduce lipoperoxidation in erythrocytes [79–81]. The importance of polyamines during erythropoiesis was also previously demonstrated by other research groups [78,82]. In line with this, inhibition of polyamine synthesis by blockage of *ODC* via difluormethyl-ornithine (DFMO) reduced erythroid expansion rates and *HBB* expression (Figure 4B,C). DC and neutrophils, in contrast, were not affected by *ODC* inhibition (Figure 3A,D). Therefore, polyamine synthesis seems solely crucial for erythropoiesis, at least in the myeloid branch of hematopoiesis. As yet, however, it is not exactly clear which of the stated functions of polyamines is eventually crucial for erythropoiesis; we assume that all of them might be crucial for different stages during erythropoiesis.

Interestingly, we found the expression of *OAT* solely increased during erythropoiesis (Table 2). *OAT* catalyzes the generation of Glu and glutamate-5-semialdehyde from Orn and aKG and vice versa [83]. Under most conditions, *OAT* uses Orn for anabolism of Glu and, therefore, belongs to the "glutamate crossway". Under certain conditions, however, *OAT* can switch to Orn synthesis. As Glu remained unchanged and Orn was raised during erythropoiesis, we, however, conclude that the favored reaction is Glu anabolism. In line with this, it has been shown that erythropoiesis is sustained during depletion of extracellular Gln, but is dependent on the intracellular synthesis from Glu under these conditions [45].

In order to evaluate the influence of *OAT* on erythropoiesis, as well as the direction of the conversion, we used 5-fluoromethylornithine (5-FMO), a specific inhibitor of *OAT* [84]. Surprisingly, addition of 5-FMO led to a reduced expression of *HBB* independent of Gln (Figure 4E,G), whilst the expansion rate was only affected in the presence of Gln (Figure 4D,F). We therefore propose that *OAT* works in both directions, depending on the conditions; in presence of Gln *OAT* catalyzes the conversion of Glu to Orn, subsequently fueling polyamine synthesis, whilst under conditions with low Gln, *OAT* prefers the conversion of Orn to Glu, leading to constant levels of Gln for nucleotide biosynthesis (Figure 5) [45]. The homeostasis of polyamine synthesis and Gln levels is evident, as inhibition of *ODC* by DFMO leads, independent of Gln levels, to diminished *HBB* expression (Figure 4C,G). Additionally, inhibition of *OAT* in the absence of Gln also reduced *HBB* expression to similar levels as DFMO, indicating that polyamine synthesis alone is not sufficient for erythropoiesis (Figure 4G). Importantly, we found that inhibition of *OAT* or *ODC* in the absence of Gln did not influence *GPNMB* expression of DC (Figure 3B), also expression of *ELANE* by neutrophils remained unaffected by 5-FMO (Figure 3D). Therefore, *OAT* mediated homeostasis of polyamine synthesis and Gln seems to be solely crucial during erythropoiesis.

2.6. PLA2G15, PLA2G16 and Fatty Acid Levels Are Three Major Regulators of Unique Lipidomic Changes

As several uniquely changed metabolites were glycerophospholipids (GPL), we also focused on GLP metabolism. GLP need to be further subdivided in acyl-acyl species (acyl glycerophospholipids, aGPL) and acyl-alkyl species (ether lipids, EL), as the former are involved in glycerophospholipid metabolism and the latter are involved in ether lipid metabolism. Interestingly, the different GPL classes (e.g., phosphatidylcholine (PC), phosphatidylethanolamine (PE) and phosphatidylserine (PS)) followed the same trend in all lineages (not shown). However, erythrocytes displayed increased aGPL levels, DC showed lowered aGPL levels and higher EL levels, while neutrophils exhibited reduced aGPL levels, in comparison to the progenitor population (Figure 2 A,B, Supplemental Tables S5–S7). Furthermore, percentual content of EL was elevated in DC and neutrophils (Figure 4A), as also reported previously [85].

We found several changes in the expression of enzymes, related to glycerophospholipid and ether lipid metabolism (Table 2); however, only *PLA2G15*, *PLA2G16*, *LPCAT3*, *PISD*, *PHOSPHO1* and *LPIN1* were affected distinctively in the corresponding populations. Furthermore, the activity of *PLBD1*, *PLD3* and *PISD* has been reported as negligible, which was also reflected by the corresponding metabolic changes [86–89]. As we found enhanced de novo FA synthesis and elongation in erythrocytes, as well as stimulated lipolysis in DC and neutrophils, the unique metabolite patterns apparently partially reflected available FA levels, as longer aGPLs were raised in erythrocytes. In DC and neutrophils, aGPLs apparently are degraded by *PLA2G15* and *PLA2G16* [90,91]. The available FA levels are further reflected by ELs, as *FAR1/2*, the major regulator of EL biosynthesis, uses C16 and C18 acyl-CoA species as substrates [92,93]. Since C16 FA are further elongated in erythrocytes, this results in limited EL synthesis due to limited substrate availability and thus unchanged EL levels. In neutrophils, *PLA2G16* additionally reduces EL biosynthesis by inducing peroxisomal dysfunction, which results in the lack of finding of uniquely raised EL, despite their higher percentual content [91].

In line with this, we found higher levels of C16, C18 and C18:1 ceramide in DC (Figure 2B). Furthermore, expression of *SPTSSB*, well-known to stimulate serine palmitoyltransferase (*SPT*) activity,

was raised in DC and erythrocytes [94]. As *SPT* uses C18-CoA substrates, we conclude that de novo ceramide synthesis is enhanced in DC, due to higher availability of sphingosine, resulting from higher C18-CoA availability.

Taken together, our data strongly indicate that parts of the cellular lipidome analyzed here are all regulated by FA levels, in combination with the expression of *PLA2G15* or *PLA2G16*, resulting in the described unique metabolic signatures.

3. Discussion

Cellular metabolism is an essential feature of living organisms; various metabolites are involved in specialized cellular tasks, ultimately defining the function of each cell. In the context of hematopoietic stem cells, it is fully appreciated that the activity of metabolic pathways not only regulate quiescence, but also regulate commitment [63,95]. Inhibition of FAO, for example, leads to symmetric commitment of HSCs, however, neutrophil differentiation is also disturbed by inhibition of FAO. [42,43] The regulatory role of FAO, therefore, remains controversial to some extent. Furthermore, several studies have shown the importance of various metabolic pathways on differentiation of several lineages [45,46,78,96]. The lineage-specific activity of these metabolic pathways, however, remains vague, a direct metabolic comparison of distinct lineages is still missing.

The total cellular metabolism plays a fundamental role in the cellular response towards different stimuli. In the context of hematopoiesis, several different compounds are known to exert distinct effects on the different blood cell populations [15,40,97–99]. The actual mode of action underlying this lineage-specific hematotoxicity, however, often remains inconclusive. Indeed, some known hematotoxic compounds (e.g., the benzene metabolite trans, trans-muconaldehyde) were shown to exert (some of) it's toxic effects by blockage of gap junction intercellular communication via cross-linking of connexin43, rendering these unidentifiable via metabolomic screening approaches [100]. Nevertheless, involvement of the total cellular metabolism in lineage-specific effects is quite likely, rendering fundamental knowledge of the different active and inactive metabolic pathways essential, in order to understand such lineage-specific effects.

We, therefore, established an HSPC differentiation model, suitable for omics-based screening approaches, and performed metabolic and transcriptomic comparison of three myeloid lineages, regarding to the initial progenitor population. Generated populations, in fact, were not purified further, potentially leading to overlapping metabolic signatures. However, by identifying distinctively altered metabolites, we found several lineage-related active metabolic pathways, some of which have also been identified previously (e.g., polyamine synthesis in erythrocytes [78] and FAO in neutrophils [43]). Presence of other lineages is even of advantage from a toxicological point of view, as toxic effects on these can also be identified simultaneously. The corresponding mode of action, then may be identified within the dominant lineage, using omics techniques. We found that conclusions made from metabolomic and transcriptomic data are in good agreement with the results of verifying inhibitor experiments, indicating the validity of the here described approach.

We could further demonstrate that not only FAO, but also the combination of fatty acid generation and their fate is unique for each lineage. Inhibition of FAO did impair neutrophil maturation, but not formation of committed progenitors, supplementing current knowledge about FAO dependence of HSC commitment. Of note, our data also suggest that glycolysis and glutaminolysis have a substantial impact on FAO, leading to differential usage of fatty acids in each lineage. We could further demonstrate a unique and essential connection of glutamine metabolism to polyamine synthesis in erythrocytes and identify the key players in lipid remodeling during myeloid lineage commitment, namely acyl-CoA availability, *PLA2G15* and *PLA2G16*.

Our results thus connect several crucial active metabolic pathways, identified in single myeloid lineages, while also displaying their unique combination for each lineage, as well as their inactivity in the other lineages. Direct usability for hematotoxicity studies is evident, as several xenobiotic compounds are known to selectively interact with specific metabolic pathways [101–103]. Likewise,

elucidation of effects by endogenous compounds on hematopoiesis can also be achieved by usage of the here presented model, which may ultimately result in new therapy approaches. Our results also enable improved interpretation of metabolic alterations, as observed by different compounds [104–106].

Taken together, the parent paper adds significant knowledge to the understanding of differences in metabolism of distinct myeloid lineages for future studies and enables transferability of results obtained with this model to other tissues. It will further contribute to an understanding of the differential impacts of environmental or xenobiotic compounds on hematopoiesis and thus adds essential knowledge for identifying phenotype-modulating metabolites.

4. Materials and Methods

4.1. Reagents and Materials

Human CB CD34$^+$ cells were purchased from STEMCELL Technologies GmbH (Cologne, Germany). StemPro-34 SFM, IMDM and valproic acid were from Fisher Scientific (Wien, Austria). Cytokines were purchased from GeneScript (Piscataway, NJ, USA). BML-210 and stemregenin 1 (SR-1) were from ApexBio Technology LCC (Houston, TX). L-Glutamine was from Carl Roth GmbH + Co.KG (Karlsruhe, Germany). Etomoxir was from VWR International GmbH (Bruchsal, Germany). Elfornithine (DFMO) and Human male AB serum was from Sigma-Aldrich Chemie GmbH (Munich, Germany). The 5-Fluoromethylornithine (5-FMO) was from Chemspace Europe (Riga, Latvia). All antibodies were purchased from Beckton Dickinson GmbH (Heidelberg, Germany).

4.2. Flow Cytometry Analyses and Antibodies

All flow cytometry data were acquired on a CyFlow Cube 8 flow cytometer (Sysmex) and analyzed using FCS Express software (De Novo Software). Cells were washed twice with PBS and blocked with 10% human male AB serum for 15 min at 4 °C. The following are the antihuman antibodies used: CD34-allophycocyanin (APC), CD38-fluorescein isothiocyanate (FITC), CD45RA-APC, CD135-phycoerythin (PE), CD71-FITC, CD235a-APC, CD3-APC, CD94-FITC, CD41-APC, CD42a-FITC, CD90-FITC, CD66b-FITC, CD14-Pacific Blue (Pac Blue) and CD1a-APC, FITC-, PE-, APC- or Pac Blue-conjugated isotype-matched antibodies served as controls.

4.3. Human CD34$^+$ Cell Culture

CD34$^+$ cells were thawed according to the vendors protocol and expanded in Stempro-34 SFM media containing 2 mM L-glutamine, 100 ng/mL SCF, 100 ng/mLFlt-3L, 50 ng/mL IL-6, 40 ng/mL TPO, 1 µM SR-1, 0.1 µM BML-210 and 0.2 mM valproic acid for 13 days [51]. Until day 8, each second day 5 mL fresh media was added to the culture. From day 9 to 13, cells were diluted 1:1 each day by addition of fresh media. Erythroid differentiation was performed in Stempro-34 SFM media containing 2 mM L-glutamine, 100 ng/mL SCF, 100 ng/mL Flt-3L, 50 ng/mL EPO and 20 ng/mL IL-3 for a total of 6 days [53]. Cells were diluted 2:3 on day 4 by addition of fresh media. DC differentiation was done in Stempro-34 SFM media containing 2 mM L-glutamine, 10 ng/mL SCF, 10 ng/mL TPO and 10 ng/mL IL-3 for a total of 11 days. Neutrophil differentiation was done in IMDM containing 10% FBS, 50 ng/mL SCF and 50 ng/mL IL-15 for a total of 10 days. Dendritic cells and neutrophils were diluted 2:3 on day 3 and 7 by addition of fresh media. Different inhibitors were added as indicated at the beginning of each differentiation and held constant during the experiment, the added volume did not exceed 0.1% (*v*/*v*).

4.4. Total RNA Isolation and RNA-Seq

Total RNA isolation was performed using the NucleoSpin RNA XS Kit (Macherey-Nagel GmbH & Co. KG). Purification of poly-A containing mRNA molecules followed by mRNA fragmentation, random primed cDNA synthesis and single read 50 bp sequencing, as well as transcriptome alignment and determination of differential expression levels were done by Eurofins GATC Biotech GmbH (Constance, Germany) [107].

4.5. Quantitative PCR Primer

HBB: fw: 5′-CTCGCTTTCTTGCTGTCCA-3′, rv: 5′-CAAGGCCCTTCATAATATCCCC-3′; ELANE: fw: 5′-CTGCGTGGCGAATGTAAACG-3′, rv: 5′-CGTTGAGCAAGTTTACGGGG-3′; GPNMB: fw: 5′-CTGATCTCCGTTGGCTGCTT-3′, rv: 5′-CTGACCACATTCCCAGGACT-3′; S100A8: fw: 5′-GATAAAGATGGGCGTGGCAG-3′, rv: 5′-TGCAGGTACATGTCCAGGG-3′; RPLP0: fw: 5′-TGGCAATCCCTGACGCACCG-3′; rv: 5′-TGCCCATCAGCACCACAGCC-3′.

4.6. LC/MS-based Metabolomics

Metabolite measurement was performed using a 4000 QTRAP mass spectrometer (ABI Sciex), connected to a NexteraXR HPLC (Shimadzu). Cell pellets were washed twice with ice-cold PBS and the pellets were resuspended at 1×10^7 cells/ml in −20 °C cold ethanol containing 15% (*v*/*v*) 10 mM K_2PO_4, pH 7.5, sonicated for 3 min and frozen in liquid nitrogen for 30 seconds. The sonication-freeze cycle was repeated twice, afterwards, samples were centrifuged at 31,500 rcf at 2 °C for 5 min and the supernatant was stored at −80 °C until measurement. The metabolome analyses were carried out using the AbsoluteIDQ p180 Kit (Biocrates Life Science AG), according to the manufacturer's instructions. Analysis of additional lipids, covering 162 glycerophospholipids, 33 sphingomyelins and 131 ceramides was done by Biocrates Life Sciences AG (Innsbruck, Austria).

4.7. Bioinformatic Analysis

Statistical analysis of metabolomics data using an empirical Bayes approach was done by using the statistical software R [108] and the bioconductor package limma [109]. Metabolite concentrations were $\log_2$ transformed prior to statistical analysis, resulting "-Infinitive" values from metabolites below the LOD were removed from the data frame. Absolute $\log_2$ fold changes (logFC) above 1, compared to the progenitor population, with a corresponding FDR-adjusted *p* value below 0.05 where considered relevant. From these, unique metabolites were defined by a $\Delta\text{logFC} > 1$ to both other lineages. As ΔlogFC, we defined the absolute difference in the logFCs from each lineage compared to the progenitor population. Common metabolites of two lineages were defined as owning a $\Delta\text{logFC} < 1$, whilst both owning a ΔlogFC compared to third lineage > 1, from the relevant set of metabolites. Common metabolites of all lineages were defined as Δ logFC < 1 between all lineages from the relevant set of metabolites. Gene Ontology enrichment analysis (Overrepresentation Test) was done by using the PANTHER Software (http://pantherdb.org), using the Fisher's Exact test type in combination with Holm adjusted *p* value [110,111]. Significant changes were assessed by a one-way ANOVA, where a *p* value smaller than 0.05 was considered as significant. For metabolic pathway visualization, using KEGG pathways as template, the software PathViso [77,112] was used.

4.8. Data Availability

RNA sequencing datasets generated are available at GEO under the accession number GSE129993. A list of identified significant altered metabolites can be found in the supplementary materials.

Supplementary Materials: Supplementary materials can be found at http://www.mdpi.com/1422-0067/21/17/6092/s1.

Author Contributions: Conceptualization, H.-P.D. and M.J.; methodology, H.-P.D. and L.K.; software, L.K. and M.K.; validation, L.K., M.B. and H.-P.D.; formal analysis, L.K.; investigation, L.K., H.W. and I.Q.; resources, H.-P.D., M.K.; data curation, L.K.; writing—original draft preparation, L.K. and H.-P.D.; writing—review and editing, L.K., M.B., M.J., R.C., M.K. and H.-P.D; visualization, L.K.; supervision, H.-P.D. and M.J.; project administration, H.-P.D.; funding acquisition, H.-P.D. All authors have read and agreed to the published version of the manuscript.

Funding: This work was supported by a scholarship for Lars Kaiser from the Federal Ministry of Science, Research and Art of Baden-Württemberg, support from the Steinbeis Center for Personalized Medicine (StZ1789) is gratefully acknowledged. MJ thanks the German Research Foundation (DFG) under Germany's Excellence Strategy (CIBSS – EXC-2189 – Project ID 390939984) for support.

Conflicts of Interest: The authors declare no conflict of interest.

Abbreviations

5-FMO	5-fluoromethylornithine
aGPL	Acyl Glycerophospholipids
CD	Cluster of differentiation
CE	Cholesteryl esters
CFU	Colony forming unit
DC	Dendritic cells
DFMO	Difluormethyl-ornithine
EL	Ether lipids
EPO	Erythropoietin
F6P	Fructose-6-phosphate
FAO	Fatty acid oxidation
FA	Fatty acids
FDR	False Discovery Rate
G6P	Glucose-6-phosphate
GPL	Glycerophospholipids
HSC	Hematopoietic stem cell
HSPC	Hematopoietic stem and progenitor cells
PC	Phosphatidylcholine
PE	Phosphatidylethanolamine
PS	Phosphatidylserine
PPP	Pentose phosphate pathway
ROS	Reactive oxygen species
TG	Triglycerides

References

1. Hunt, P.R. The *C. elegans* model in toxicity testing. *J. Appl. Toxicol.* **2017**, *37*, 50–59. [CrossRef]
2. Miranda, J.P.; Leite, S.B.; Muller-Vieira, U.; Rodrigues, A.; Carrondo, M.J.T.; Alves, P.M. Towards an extended functional hepatocyte in vitro culture. *Tissue Eng. Part C Methods* **2009**, *15*, 157–167. [CrossRef] [PubMed]
3. Bhattacharya, S.; Zhang, Q.; Carmichael, P.L.; Boekelheide, K.; Andersen, M.E. Toxicity testing in the 21st century: Defining new risk assessment approaches based on perturbation of intracellular toxicity pathways. *PLoS ONE* **2011**, *6*. [CrossRef] [PubMed]
4. Bradley, E.L.; Honkalampi-Hämäläinen, U.; Weber, A.; Andersson, M.A.; Bertaud, F.; Castle, L.; Dahlman, O.; Hakulinen, P.; Hoornstra, D.; Lhuguenot, J.C.; et al. The BIOSAFEPAPER project for in vitro toxicity assessments: Preparation, detailed chemical characterisation and testing of extracts from paper and board samples. *Food Chem. Toxicol.* **2008**, *46*, 2498–2509. [CrossRef] [PubMed]
5. Lipman, J.; Flint, O.; Bradlaw, J.; Frazier, J. Cell culture systems and in vitro toxicity testing. In *Animals and Alternatives in Testing: History, Science and Ethics*; Kluwer Academic Publishers: Dordrecht, The Netherlands, 1990; Volume 8, pp. 129–176.
6. Moya, M.L.; Hsu, Y.H.; Lee, A.P.; Christopher, C.W.H.; George, S.C. In vitro perfused human capillary networks. *Tissue Eng. Part C Methods* **2013**, *19*, 730–737. [CrossRef] [PubMed]
7. Garrod, M.; Chau, D.Y.S. An overview of tissue engineering as an alternative for toxicity assessment. *J. Pharm. Pharm. Sci.* **2016**, *19*, 31–71. [CrossRef]
8. Pupovac, A.; Senturk, B.; Griffoni, C.; Maniura-Weber, K.; Rottmar, M.; McArthur, S.L. Toward Immunocompetent 3D Skin Models. *Adv. Healthc. Mater.* **2018**, *7*. [CrossRef] [PubMed]
9. Mahler, G.J.; Esch, M.B.; Stokol, T.; Hickman, J.J.; Shuler, M.L. Body-on-A-Chip systems for Animal-free toxicity testing. *ATLA Altern. to Lab. Anim.* **2016**, *44*, 469–478. [CrossRef] [PubMed]
10. Luz, A.L.; Tokar, E.J. Pluripotent Stem Cells in Developmental Toxicity Testing: A Review of Methodological Advances. *Toxicol. Sci.* **2018**, *165*, 31–39. [CrossRef]
11. Anson, B.D.; Kolaja, K.L.; Kamp, T.J. Opportunities for use of human iPS cells in predictive toxicology. *Clin. Pharmacol. Ther.* **2011**, *89*, 754–758. [CrossRef]

12. Scott, C.W.; Peters, M.F.; Dragan, Y.P. Human induced pluripotent stem cells and their use in drug discovery for toxicity testing. *Toxicol. Lett.* **2013**, *219*, 49–58. [CrossRef] [PubMed]
13. Balls, M.; Combes, R.D.; Bhogal, N. (Eds.) *New Technologies for Toxicity Testing*; Advances in Experimental Medicine and Biology; Springer US: New York, NY, USA, 2012; Volume 745, ISBN 978-1-4614-3054-4.
14. Laiosa, M.D.; Tate, E.R. Fetal hematopoietic stem cells are the canaries in the coal mine that portend later life immune deficiency. *Endocrinology* **2015**, *156*, 3458–3465. [CrossRef] [PubMed]
15. Van Den Heuvel, R.L.; Leppens, H.; Schoeters, G.E.R. Use of in vitro assays to assess hematotoxic effects of environmental compounds. *Cell Biol. Toxicol.* **2001**, *17*, 107–116. [CrossRef] [PubMed]
16. Mahalingaiah, P.K.; Palenski, T.; Van Vleet, T.R. An In Vitro Model of Hematotoxicity: Differentiation of Bone Marrow–Derived Stem/Progenitor Cells into Hematopoietic Lineages and Evaluation of Lineage-Specific Hematotoxicity. *Curr. Protoc. Toxicol.* **2018**, *76*, e45. [CrossRef] [PubMed]
17. Owen, L.; Laird, K.; Wilson, P.B. Structure-activity modelling of essential oils, their components, and key molecular parameters and descriptors. *Mol. Cell. Probes* **2018**, *38*, 25–30. [CrossRef]
18. Uehara, T.; Hirode, M.; Ono, A.; Kiyosawa, N.; Omura, K.; Shimizu, T.; Mizukawa, Y.; Miyagishima, T.; Nagao, T.; Urushidani, T. A toxicogenomics approach for early assessment of potential non-genotoxic hepatocarcinogenicity of chemicals in rats. *Toxicology* **2008**, *250*, 15–26. [CrossRef]
19. Duke, S.O.; Bajsa, J.; Pan, Z. Omics Methods for Probing the Mode of Action of Natural and Synthetic Phytotoxins. *J. Chem. Ecol.* **2013**, *39*, 333–347. [CrossRef]
20. Ramirez, T.; Strigun, A.; Verlohner, A.; Huener, H.A.; Peter, E.; Herold, M.; Bordag, N.; Mellert, W.; Walk, T.; Spitzer, M.; et al. Prediction of liver toxicity and mode of action using metabolomics in vitro in HepG2 cells. *Arch. Toxicol.* **2018**, *92*, 893–906. [CrossRef]
21. Labine, L.M.; Simpson, M.J. The use of nuclear magnetic resonance (NMR) and mass spectrometry (MS)–based metabolomics in environmental exposure assessment. *Curr. Opin. Environ. Sci. Heal.* **2020**, *15*, 7–15. [CrossRef]
22. Emwas, A.H.M. The strengths and weaknesses of NMR spectroscopy and mass spectrometry with particular focus on metabolomics research. *Methods Mol. Biol.* **2015**, *1277*, 161–193. [CrossRef]
23. Potratz, S.; Tarnow, P.; Jungnickel, H.; Baumann, S.; Von Bergen, M.; Tralau, T.; Luch, A. Combination of Metabolomics with Cellular Assays Reveals New Biomarkers and Mechanistic Insights on Xenoestrogenic Exposures in MCF-7 Cells. *Chem. Res. Toxicol.* **2017**, *30*, 883–892. [CrossRef] [PubMed]
24. Lorenz, M.A.; Burant, C.F.; Kennedy, R.T. Reducing time and increasing sensitivity in sample preparation for adherent mammalian cell metabolomics. *Anal. Chem.* **2011**, *83*, 3406–3414. [CrossRef] [PubMed]
25. Srivastava, A.; Evans, K.J.; Sexton, A.E.; Schofield, L.; Creek, D.J. Metabolomics-Based Elucidation of Active Metabolic Pathways in Erythrocytes and HSC-Derived Reticulocytes. *J. Proteome Res.* **2017**, *16*, 1492–1505. [CrossRef] [PubMed]
26. Sapcariu, S.C.; Kanashova, T.; Weindl, D.; Ghelfi, J.; Dittmar, G.; Hiller, K. Simultaneous extraction of proteins and metabolites from cells in culture. *MethodsX* **2014**, *1*, 74–80. [CrossRef] [PubMed]
27. Muschet, C.; Möller, G.; Prehn, C.; de Angelis, M.H.; Adamski, J.; Tokarz, J. Removing the bottlenecks of cell culture metabolomics: Fast normalization procedure, correlation of metabolites to cell number, and impact of the cell harvesting method. *Metabolomics* **2016**, *12*, 1–12. [CrossRef] [PubMed]
28. Kubyshkin, V.; Budisa, N. Amide rotation trajectories probed by symmetry. *Org. Biomol. Chem.* **2017**, *15*, 6764–6772. [CrossRef]
29. Grootveld, M.; Percival, B.; Gibson, M.; Osman, Y.; Edgar, M.; Molinari, M.; Mather, M.L.; Casanova, F.; Wilson, P.B. Progress in low-field benchtop NMR spectroscopy in chemical and biochemical analysis. *Anal. Chim. Acta* **2019**, *1067*, 11–30. [CrossRef]
30. Chen, C.; Fan, Z.; Xu, H.; Tan, X.; Zhu, M. Metabolomics-based parallel discovery of xenobiotics and induced endogenous metabolic dysregulation in clinical toxicology. *Biomed. Chromatogr.* **2019**, *33*, e4413. [CrossRef]
31. Ortmayr, K.; Dubuis, S.; Zampieri, M. Metabolic profiling of cancer cells reveals genome-wide crosstalk between transcriptional regulators and metabolism. *Nat. Commun.* **2019**, *10*, 1–13. [CrossRef]
32. Leenders, J.; Grootveld, M.; Percival, B.; Gibson, M.; Casanova, F.; Wilson, P.B. Benchtop low-frequency 60 MHz NMR analysis of urine: A comparative metabolomics investigation. *Metabolites* **2020**, *10*, 155. [CrossRef]
33. Patel, C.H.; Leone, R.D.; Horton, M.R.; Powell, J.D. Targeting metabolism to regulate immune responses in autoimmunity and cancer. *Nat. Rev. Drug Discov.* **2019**, *18*, 669–688. [CrossRef] [PubMed]

34. Zhang, S.; Carriere, J.; Lin, X.; Xie, N.; Feng, P. Interplay between cellular metabolism and cytokine responses during viral infection. *Viruses* **2018**, *10*, 521. [CrossRef] [PubMed]
35. Qu, Q.; Zeng, F.; Liu, X.; Wang, Q.J.; Deng, F. Fatty acid oxidation and carnitine palmitoyltransferase I: Emerging therapeutic targets in cancer. *Cell Death Dis.* **2016**, *7*, e2226. [CrossRef] [PubMed]
36. Quijano, C.; Trujillo, M.; Castro, L.; Trostchansky, A. Interplay between oxidant species and energy metabolism. *Redox Biol.* **2016**, *8*, 28–42. [CrossRef] [PubMed]
37. Scheding, S.; Loeffler, M.; Schmitz, S.; Seidel, H.J.; -Erich Wichmann, H. Hematotoxic effects of benzene analyzed by mathematical modeling. *Toxicology* **1992**, *72*, 265–279. [CrossRef]
38. Nagata, M.; Arimitsu, N.; Ito, T.; Sekimizu, K. Antioxidant N-acetyl-l-cysteine inhibits erythropoietin-induced differentiation of erythroid progenitors derived from mouse fetal liver. *Cell Biol. Int.* **2007**, *31*, 252–256. [CrossRef]
39. Zembron-Lacny, A.; Slowinska-Lisowska, M.; Szygula, Z.; Witkowski, Z.; Szyszka, K. Modulatory effect of N-acetylcysteine on pro-antioxidant status and haematological response in healthy men. *J. Physiol. Biochem.* **2010**, *66*, 15–21. [CrossRef]
40. Scheding, S.; Media, J.E.; Nakeff, A. Acute toxic effects of 3′-azido-3′-deoxythymidine (AZT) on normal and regenerating murine hematopoiesis. *Exp. Hematol.* **1994**, *22*, 60–65.
41. Luo, S.T.; Zhang, D.M.; Qin, Q.; Lu, L.; Luo, M.; Guo, F.C.; Shi, H.S.; Jiang, L.; Shao, B.; Li, M.; et al. The Promotion of Erythropoiesis via the Regulation of Reactive Oxygen Species by Lactic Acid. *Sci. Rep.* **2017**, *7*, 38105. [CrossRef]
42. Ito, K.; Carracedo, A.; Weiss, D.; Arai, F.; Ala, U.; Avigan, D.E.; Schafer, Z.T.; Evans, R.M.; Suda, T.; Lee, C.-H.; et al. A PML–PPAR-δ pathway for fatty acid oxidation regulates hematopoietic stem cell maintenance. *Nat. Med.* **2012**, *18*, 1350–1358. [CrossRef]
43. Riffelmacher, T.; Clarke, A.; Richter, F.C.; Stranks, A.; Pandey, S.; Danielli, S.; Hublitz, P.; Yu, Z.; Johnson, E.; Schwerd, T.; et al. Autophagy-Dependent Generation of Free Fatty Acids Is Critical for Normal Neutrophil Differentiation. *Immunity* **2017**, *47*, 466–480.e5. [CrossRef] [PubMed]
44. Cruzat, V.; Macedo Rogero, M.; Noel Keane, K.; Curi, R.; Newsholme, P. Glutamine: Metabolism and Immune Function, Supplementation and Clinical Translation. *Nutrients* **2018**, *10*, 1564. [CrossRef] [PubMed]
45. Oburoglu, L.; Tardito, S.; Fritz, V.; De Barros, S.C.; Merida, P.; Craveiro, M.; Mamede, J.; Cretenet, G.; Mongellaz, C.; An, X.; et al. Glucose and Glutamine Metabolism Regulate Human Hematopoietic Stem Cell Lineage Specification. *Cell Stem Cell* **2014**, *15*, 169–184. [CrossRef] [PubMed]
46. Huang, N.J.; Lin, Y.C.; Lin, C.Y.; Pishesha, N.; Lewis, C.A.; Freinkman, E.; Farquharson, C.; Millán, J.L.; Lodish, H. Enhanced phosphocholine metabolism is essential for terminal erythropoiesis. *Blood* **2018**, *131*, 2955–2966. [CrossRef] [PubMed]
47. Niskanen, E.; Kallio, A.; McCann, P.P.; Baker, D.G. The role of polyamine biosynthesis in hematopoietic precursor cell proliferation in mice. *Blood* **1983**, *61*, 740–745. [CrossRef]
48. Segal, G.M.; Stueve, T.; Adamson, J.W. Spermine and spermidine are non-specific inhibitors of in vitro hematopoiesis. *Kidney Int.* **1987**, *31*, 72–76. [CrossRef] [PubMed]
49. Miller-Fleming, L.; Olin-Sandoval, V.; Campbell, K.; Ralser, M. Remaining Mysteries of Molecular Biology: The Role of Polyamines in the Cell. *J. Mol. Biol.* **2015**, *427*, 3389–3406. [CrossRef]
50. Kaiser, L.; Weinschrott, H.; Quint, I.; Csuk, R.; Jung, M.; Deigner, H.-P. Fatty acid oxidation makes the difference: Lineage-selective disturbance by DEHP via ROS in myeloid hematopoiesis. *bioRxiv* **2020**. [CrossRef]
51. Wang, L.; Guan, X.; Wang, H.; Shen, B.; Zhang, Y.; Ren, Z.; Ma, Y.; Ding, X.; Jiang, Y. A small-molecule/cytokine combination enhances hematopoietic stem cell proliferation via inhibition of cell differentiation. *Stem Cell Res. Ther.* **2017**, *8*, 169. [CrossRef]
52. Manz, M.G.; Miyamoto, T.; Akashi, K.; Weissman, I.L. Prospective isolation of human clonogenic common myeloid progenitors. *Proc. Natl. Acad. Sci. USA* **2002**, *99*, 11872–11877. [CrossRef]
53. Zhang, Y.; Wang, C.; Wang, L.; Shen, B.; Guan, X.; Tian, J.; Ren, Z.; Ding, X.; Ma, Y.; Dai, W.; et al. Large-Scale Ex Vivo Generation of Human Red Blood Cells from Cord Blood CD34 + Cells. *Stem Cells Transl. Med.* **2017**, 1–12. [CrossRef] [PubMed]
54. Miyazaki, R.; Ogata, H.; Iguchi, T.; Sogo, S.; Kushida, T.; Ito, T.; Inaba, M.; Ikehara, S.; Kobayashi, Y. Comparative analyses of megakaryocytes derived from cord blood and bone marrow. *Br. J. Haematol.* **2000**, *108*, 602–609. [CrossRef]

55. Woo, S.-Y.; Jung, Y.-J.; Ryu, K.-H.; Park, H.-Y.; Kie, J.-H.; Im, S.-A.; Chung, W.-S.; Han, H.-S.; Seoh, J.-Y. In vitro differentiation of natural killer T cells from human cord blood CD34+ cells. *Br. J. Haematol.* **2003**, *121*, 148–156. [CrossRef] [PubMed]
56. Gutknecht, M.; Geiger, J.; Joas, S.; Dörfel, D.; Salih, H.R.; Müller, M.R.; Grünebach, F.; Rittig, S.M. The transcription factor MITF is a critical regulator of GPNMB expression in dendritic cells. *Cell Commun. Signal.* **2015**, *13*, 19. [CrossRef]
57. Van Schaarenburg, R.A.; Suurmond, J.; Habets, K.L.L.; Brouwer, M.C.; Wouters, D.; Kurreeman, F.A.S.; Huizinga, T.W.J.; Toes, R.E.M.; Trouw, L.A. The production and secretion of complement component C1q by human mast cells. *Mol. Immunol.* **2016**, *78*, 164–170. [CrossRef] [PubMed]
58. Gliddon, D.R.; Howard, C.J. CD26 is expressed on a restricted subpopulation of dendritic cells in vivo. *Eur. J. Immunol.* **2002**, *32*, 1472. [CrossRef]
59. Zimmerman, A.W.; Joosten, B.; Torensma, R.; Parnes, J.R.; van Leeuwen, F.N.; Figdor, C.G. Long-term engagement of CD6 and ALCAM is essential for T-cell proliferation induced by dendritic cells. *Blood* **2006**, *107*, 3212–3220. [CrossRef]
60. Tessier Carle Ryckman, P.A.; Vandal, K.; Rouleau, P. Neutrophil Chemotaxis and Adhesion S100A8, S100A9, and S100A8/A9 Induce Proinflammatory Activities of S100: Proteins. *J Immunol Ref.* **2003**, *170*, 3233–3242. [CrossRef]
61. Berg, J.M.; Tymoczko, J.L.; Stryer, L. The Glycolytic Pathway Is Tightly Controlled. In *Biochemistry*, 5th ed.; W H Freeman: New York, NY, USA, 2002; ISBN 978-0716746843.
62. Lieberman, M.D.; Cunningham, W.A. Type I and Type II error concerns in fMRI research: Re-balancing the scale. *Soc. Cogn. Affect. Neurosci.* **2009**, *4*, 423–428. [CrossRef]
63. Oburoglu, L.; Romano, M.; Taylor, N.; Kinet, S. Metabolic regulation of hematopoietic stem cell commitment and erythroid differentiation. *Curr. Opin. Hematol.* **2016**, *23*, 198–205. [CrossRef]
64. Borregaard, N.; Herlin, T. Energy metabolism of human neutrophils during phagocytosis. *J. Clin. Investig.* **1982**, *70*, 550–557. [CrossRef]
65. Kelly, B.; O'Neill, L.A.J. Metabolic reprogramming in macrophages and dendritic cells in innate immunity. *Cell Res.* **2015**, *25*, 771–784. [CrossRef] [PubMed]
66. Fiamoncini, J.; Lima, T.M.; Hirabara, S.M.; Ecker, J.; Gorjão, R.; Romanatto, T.; Elolimy, A.; Worsch, S.; Laumen, H.; Bader, B.; et al. Medium-chain dicarboxylic acylcarnitines as markers of n-3 PUFA-induced peroxisomal oxidation of fatty acids. *Mol. Nutr. Food Res.* **2015**, *59*, 1573–1583. [CrossRef] [PubMed]
67. McCoin, C.S.; Knotts, T.A.; Adams, S.H. Acylcarnitines–old actors auditioning for new roles in metabolic physiology. *Nat. Rev. Endocrinol.* **2015**, *11*, 617–625. [CrossRef] [PubMed]
68. Reuter, S.E.; Evans, A.M. Carnitine and Acylcarnitines. *Clin. Pharmacokinet.* **2012**, *51*, 553–572. [CrossRef]
69. Su, X.; Han, X.; Mancuso, D.J.; Abendschein, D.R.; Gross, R.W. Accumulation of long-chain acylcarnitine and 3-hydroxy acylcarnitine molecular species in diabetic myocardium: Identification of alterations in mitochondrial fatty acid processing in diabetic myocardium by shotgun lipidomics. *Biochemistry* **2005**, *44*, 5234–5245. [CrossRef]
70. Wanders, R.J.A.; Komen, J.; Kemp, S. Fatty acid omega-oxidation as a rescue pathway for fatty acid oxidation disorders in humans. *FEBS J.* **2011**, *278*, 182–194. [CrossRef]
71. Jansen, G.A.; Wanders, R.J.A. Alpha-Oxidation. *Biochim. Biophys. Acta Mol. Cell Res.* **2006**, *1763*, 1403–1412. [CrossRef]
72. Grassi, L.; Pourfarzad, F.; Ullrich, S.; Merkel, A.; Were, F.; Carrillo-de-Santa-Pau, E.; Yi, G.; Hiemstra, I.H.; Tool, A.T.J.; Mul, E.; et al. Dynamics of Transcription Regulation in Human Bone Marrow Myeloid Differentiation to Mature Blood Neutrophils. *Cell Rep.* **2018**, *24*, 2784–2794. [CrossRef]
73. Evrard, M.; Kwok, I.W.H.; Chong, S.Z.; Teng, K.W.W.; Becht, E.; Chen, J.; Sieow, J.L.; Penny, H.L.; Ching, G.C.; Devi, S.; et al. Developmental Analysis of Bone Marrow Neutrophils Reveals Populations Specialized in Expansion, Trafficking, and Effector Functions. *Immunity* **2018**, *48*, 364–379.e8. [CrossRef]
74. Kim, M.H.; Yang, D.; Kim, M.; Kim, S.Y.; Kim, D.; Kang, S.J. A late-lineage murine neutrophil precursor population exhibits dynamic changes during demand-adapted granulopoiesis. *Sci. Rep.* **2017**, *7*, 39804. [CrossRef]
75. Cassago, A.; Ferreira, A.P.S.; Ferreira, I.M.; Fornezari, C.; Gomes, E.R.M.; Greene, K.S.; Pereira, H.M.; Garratt, R.C.; Dias, S.M.G.; Ambrosio, A.L.B. Mitochondrial localization and structure-based phosphate activation mechanism of Glutaminase C with implications for cancer metabolism. *Proc. Natl. Acad. Sci. USA* **2012**, *109*, 1092–1097. [CrossRef] [PubMed]

76. He, Z.; Zhu, X.; Shi, Z.; Wu, T.; Wu, L. Metabolic Regulation of Dendritic Cell Differentiation. *Front. Immunol.* **2019**, *10*, 410. [CrossRef]
77. Kanehisa, M. KEGG: Kyoto Encyclopedia of Genes and Genomes. *Nucleic Acids Res.* **2000**, *28*, 27–30. [CrossRef] [PubMed]
78. Maeda, T.; Wakasawa, T.; Shima, Y.; Tsuboi, I.; Aizawa, S.; Tamai, I. Role of Polyamines Derived from Arginine in Differentiation and Proliferation of Human Blood Cells. *Biol. Pharm. Bull.* **2006**, *29*, 234–239. [CrossRef] [PubMed]
79. Ballas, S.K.; Mohandas, N.; Marton, L.J.; Shohet, S.B. Stabilization of erythrocyte membranes by polyamines. *Proc. Natl. Acad. Sci. USA* **2006**, *80*, 1942–1946. [CrossRef]
80. Bratton, D.L. Polyamine inhibition of transbilayer movement of plasma membrane phospholipids in the erythrocyte ghost. *J. Biol. Chem.* **1994**, *269*, 22517–22523.
81. Farriol, M.; Segovia-Silvestre, T.; Venereo, Y.; Orta, X. Antioxidant effect of polyamines on erythrocyte cell membrane lipoperoxidation after free-radical damage. *Phytother. Res.* **2003**, *17*, 44–47. [CrossRef]
82. Shima, Y.; Maeda, T.; Aizawa, S.; Tsuboi, I.; Kobayashi, D.; Kato, R.; Tamai, I. L-arginine import via cationic amino acid transporter CAT1 is essential for both differentiation and proliferation of erythrocytes. *Blood* **2006**, *107*, 1352–1356. [CrossRef]
83. Ginguay, A.; Cynober, L.; Curis, E.; Nicolis, I. Ornithine Aminotransferase, an Important Glutamate-Metabolizing Enzyme at the Crossroads of Multiple Metabolic Pathways. *Biology* **2017**, *6*, 18. [CrossRef]
84. Daune, G.; Gerhart, F.; Seiler, N. 5-Fluoromethylornithine, an irreversible and specific inhibitor of l-ornithine:2-oxo-acid aminotransferase. *Biochem. J.* **1988**, *253*, 481–488. [CrossRef] [PubMed]
85. Dean, J.M.; Lodhi, I.J. Structural and functional roles of ether lipids. *Protein Cell* **2018**, *9*, 196–206. [CrossRef] [PubMed]
86. Gavin, A.L.; Huang, D.; Huber, C.; Mårtensson, A.; Tardif, V.; Skog, P.D.; Blane, T.R.; Thinnes, T.C.; Osborn, K.; Chong, H.S.; et al. PLD3 and PLD4 are single-stranded acid exonucleases that regulate endosomal nucleic-acid sensing. *Nat. Immunol.* **2018**, *19*, 942–953. [CrossRef] [PubMed]
87. Xu, S.; Zhao, L.; Larsson, A.; Venge, P. The identification of a phospholipase B precursor in human neutrophils. *FEBS J.* **2009**, *276*, 175–186. [CrossRef] [PubMed]
88. Voelker, D.R. Phosphatidylserine decarboxylase. *Biochim. Biophys. Acta Lipids Lipid Metab.* **1997**, *1348*, 236–244. [CrossRef]
89. McMaster, C.R.; Bell, R.M. CDP-ethanolamine:1,2-diacylglycerol ethanolaminephosphotransferase. *Biochim. Biophys. Acta Lipids Lipid Metab.* **1997**, *1348*, 117–123. [CrossRef]
90. Glukhova, A.; Hinkovska-Galcheva, V.; Kelly, R.; Abe, A.; Shayman, J.A.; Tesmer, J.J.G.G. Structure and function of lysosomal phospholipase A2 and lecithin:cholesterol acyltransferase. *Nat. Commun.* **2015**, *6*, 6250. [CrossRef]
91. Uyama, T.; Ichi, I.; Kono, N.; Inoue, A.; Tsuboi, K.; Jin, X.-H.H.; Araki, N.; Aoki, J.; Arai, H.; Ueda, N. Regulation of peroxisomal lipid metabolism by catalytic activity of tumor suppressor H-rev107. *J. Biol. Chem.* **2012**, *287*, 2706–2718. [CrossRef]
92. Cheng, J.B.; Russell, D.W. Mammalian Wax Biosynthesis I. Identification of two fatty acyl-Coenzyme A reductases with different substrate specificities and tissue distributions. *J. Biol. Chem.* **2004**, *279*, 37789–37797. [CrossRef]
93. Honsho, M.; Asaoku, S.; Fujiki, Y. Posttranslational regulation of fatty acyl-CoA reductase 1, Far1, controls ether glycerophospholipid synthesis. *J. Biol. Chem.* **2010**, *285*, 8537–8542. [CrossRef]
94. Han, G.; Gupta, S.D.; Gable, K.; Niranjanakumari, S.; Moitra, P.; Eichler, F.; Brown, R.H.; Harmon, J.M.; Dunn, T.M. Identification of small subunits of mammalian serine palmitoyltransferase that confer distinct acyl-CoA substrate specificities. *Proc. Natl. Acad. Sci. USA* **2009**, *106*, 8186–8191. [CrossRef]
95. Karigane, D.; Takubo, K. Metabolic regulation of hematopoietic and leukemic stem/progenitor cells under homeostatic and stress conditions. *Int. J. Hematol.* **2017**, *106*, 18–26. [CrossRef]
96. Du, X.; Chapman, N.M.; Chi, H. Emerging roles of cellular metabolism in regulating dendritic cell subsets and function. *Front. Cell Dev. Biol.* **2018**, *6*, 152. [CrossRef] [PubMed]
97. Wiciński, M.; Węclewicz, M.M. Clozapine-induced agranulocytosis/granulocytopenia: Mechanisms and monitoring. *Curr. Opin. Hematol.* **2018**, *25*, 22–28. [CrossRef] [PubMed]

98. Ohtoyo, M.; Machinaga, N.; Inoue, R.; Hagihara, K.; Yuita, H.; Tamura, M.; Hashimoto, R.; Chiba, J.; Muro, F.; Watanabe, J.; et al. Component of Caramel Food Coloring, THI, Causes Lymphopenia Indirectly via a Key Metabolic Intermediate. *Cell Chem. Biol.* **2016**, *23*, 555–560. [CrossRef] [PubMed]
99. Demur, C.; Métais, B.; Canlet, C.; Tremblay-Franco, M.; Gautier, R.; Blas-Y-Estrada, F.; Sommer, C.; Gamet-Payrastre, L. Dietary exposure to a low dose of pesticides alone or as a mixture: The biological metabolic fingerprint and impact on hematopoiesis. *Toxicology* **2013**, *308*, 74–87. [CrossRef] [PubMed]
100. Rivedal, E.; Leithe, E. The benzene metabolite trans, trans-muconaldehyde blocks gap junction intercellular communication by cross-linking connexin43. *Toxicol. Appl. Pharmacol.* **2008**, *232*, 463–468. [CrossRef] [PubMed]
101. Menale, C.; Mita, D.G.; Diano, N.; Diano, S. Adverse Effects of Bisphenol A Exposure on Glucose Metabolism Regulation. *Open Biotechnol. J.* **2016**, *10*, 122–130. [CrossRef]
102. Anderson, C.C.; Aivazidis, S.; Kuzyk, C.L.; Jain, A.; Roede, J.R. Acute Maneb Exposure Significantly Alters Both Glycolysis and Mitochondrial Function in Neuroblastoma Cells. *Toxicol. Sci.* **2018**, *165*, 61–73. [CrossRef]
103. Burri, L.; Bjørndal, B.; Wergedahl, H.; Berge, K.; Bohov, P.; Svardal, A.; Berge, R.K. Tetradecylthioacetic Acid Increases Hepatic Mitochondrial β-Oxidation and Alters Fatty Acid Composition in a Mouse Model of Chronic Inflammation. *Lipids* **2011**, *46*, 679–689. [CrossRef]
104. Maćczak, A.; Cyrkler, M.; Bukowska, B.; Michałowicz, J. Eryptosis-inducing activity of bisphenol A and its analogs in human red blood cells (in vitro study). *J. Hazard. Mater.* **2016**, *307*, 328–335. [CrossRef] [PubMed]
105. Olchowik-Grabarek, E.; Makarova, K.; Mavlyanov, S.; Abdullajanova, N.; Zamaraeva, M. Comparative analysis of BPA and HQ toxic impacts on human erythrocytes, protective effect mechanism of tannins (*Rhus typhina*). *Environ. Sci. Pollut. Res.* **2018**, *25*, 1200–1209. [CrossRef] [PubMed]
106. Vanherwegen, A.S.; Eelen, G.; Ferreira, G.B.; Ghesquière, B.; Cook, D.P.; Nikolic, T.; Roep, B.; Carmeliet, P.; Telang, S.; Mathieu, C.; et al. Vitamin D controls the capacity of human dendritic cells to induce functional regulatory T cells by regulation of glucose metabolism. *J. Steroid Biochem. Mol. Biol.* **2019**, *187*, 134–145. [CrossRef] [PubMed]
107. Trapnell, C.; Williams, B.A.; Pertea, G.; Mortazavi, A.; Kwan, G.; van Baren, M.J.; Salzberg, S.L.; Wold, B.J.; Pachter, L. Transcript assembly and quantification by RNA-Seq reveals unannotated transcripts and isoform switching during cell differentiation. *Nat. Biotechnol.* **2010**, *28*, 511–515. [CrossRef]
108. R Core Team. *R: A Language and Environment for Statistical Computing*; R Foundation for Statistical Computing: Vienna, Austria, 2018.
109. Ritchie, M.E.; Phipson, B.; Wu, D.; Hu, Y.; Law, C.W.; Shi, W.; Smyth, G.K. limma powers differential expression analyses for RNA-sequencing and microarray studies. *Nucleic Acids Res.* **2015**, *43*, e47. [CrossRef]
110. Mi, H.; Muruganujan, A.; Ebert, D.; Huang, X.; Thomas, P.D. PANTHER version 14: More genomes, a new PANTHER GO-slim and improvements in enrichment analysis tools. *Nucleic Acids Res.* **2019**, *47*, D419–D426. [CrossRef] [PubMed]
111. Chen, S.Y.; Feng, Z.; Yi, X. A general introduction to adjustment for multiple comparisons. *J. Thorac. Dis.* **2017**, *9*, 1725–1729. [CrossRef]
112. Kutmon, M.; van Iersel, M.P.; Bohler, A.; Kelder, T.; Nunes, N.; Pico, A.R.; Evelo, C.T. PathVisio 3: An Extendable Pathway Analysis Toolbox. *PLOS Comput. Biol.* **2015**, *11*, e1004085. [CrossRef]